[39] T. Jiang and N. D. Sidiropoulos, "Kruskal's permutation lemma and the identification of CANDECOMP/PARAFAC and bilinear models with constant modulus constraints," *IEEE Trans. Signal Process.*, vol. 52, no. 9, pp. 2625–2636, Sep. 2004.
[40] L. De Lathauwer, "A link between the canonical decomposition in multilinear algebra and simultaneous matrix diagonalization," *SIAM J. Matrix Anal. Appl.*, vol. 28, no. 3, pp. 642–666, 2006.
[41] X. Liu and N. D. Sidiropoulos, "Cramér-Rao lower bounds for low-rank decompositions of multidimensional arrays," *IEEE Trans. Signal Process.*, vol. 49, no. 9, pp. 2074–2089, Sep. 2001.
[42] T.-J. Shan, M. Wax, and T. Kailath, "On spatial smoothing for direction-of-arrival estimation of coherent signals," *IEEE Trans. Acoust., Speech, Signal Process.*, vol. 33, no. 4, pp. 806–811, Aug. 1985.
[43] N. D. Sidiropoulos and X. Liu, "Identifiability results for blind beamforming in incoherent multipath with small delay spread," *IEEE Trans. Signal Process.*, vol. 49, no. 1, pp. 228–236, Jan. 2001.

SNR Estimation in a Non-Coherent BFSK Receiver With a Carrier Frequency Offset

Syed Ali Hassan and Mary Ann Ingram

***Abstract*—This correspondence deals with the problem of estimating average signal-to-noise ratio (SNR) for a communication link employing binary frequency shift keying (BFSK) in the presence of a carrier frequency offset (CFO). The transmitted symbols are corrupted by Rayleigh fading and additive white Gaussian noise (AWGN). We treat the CFO as a nuisance parameter and estimate it using a data statistics based estimator. This estimate is then used to design a maximum likelihood (ML) estimator to get the estimates of SNR. We also derive the Cramér–Rao bound (CRB) for the estimators and have shown the performance of both the data-aided and non-data-aided estimators.**

***Index Terms*— BFSK receiver, carrier frequency offset, Rayleigh fading, SNR estimation.**

I. Introduction

Estimates of signal-to-noise ratio (SNR) are used in many wireless receiver functions, including signal detection, power control algorithms, link adaptation, and turbo decoding, etc. Furthermore, if the radios are energy constrained, e.g., if they are in a sensor network, constant envelope modulation and noncoherent demodulation are desirable to reduce circuit consumption of energy. Frequency shift keying (FSK) enables efficient power amplification in the transmitter and a simple receiver design that employs envelope detection. However, the carrier frequency offset (CFO) causes error in the estimation of SNR; this will degrade the performance of systems that depend upon the knowledge of SNR, e.g., amplify and forward (AF) cooperative algorithms [1]. Thus, in this correspondence, we estimate the SNR of a noncoherent BFSK receiver in the presence of a carrier offset, treating the CFO as a nuisance parameter. The CFO estimation problem is quite tedious to solve because of its highly nonlinear nature, hence analytical methods cannot be directly applied to solve the problem at hand. Therefore, in this correspondence we derive a maximum likelihood estimator for the SNR that uses a moment-based CFO estimator. We also derive the Cramér–Rao lower bound (CRB) for the SNR estimator. We provide two types of SNR estimators: a data-aided (DA) estimator that uses the pilot symbols and a non-data-aided (NDA) estimator that does blind estimation on the received symbols.

Several authors have attacked the problem of estimating the SNR for binary phase shift keying (BPSK) and FSK receivers under perfect synchronization conditions. For example, [2] compares a variety of techniques for SNR estimation in AWGN for M-PSK signals. Many approaches also include the channel effects such as multipath fading and address the issue of SNR estimation for fading channels for BPSK, e.g., in [3]–[6]. In [7], the authors have estimated the average SNR for noncoherent binary FSK (NCBFSK) receiver, assuming a Rayleigh fading channel and unit noise power spectral density. However, in implementations, noise power must also be estimated. The authors in [8] and [9] have derived the SNR estimators for the noncoherent MFSK receivers for Rayleigh as well as block fading channels. However, they assume perfect carrier synchronization at the receiver. The work in [10] and [11] have addressed the problem of calculating the bit error probabilities for NCFSK systems in the presence of CFO.

The rest of the correspondence is organized as follows. In the next section, we describe the system model and the notations used for the BFSK receiver operating in the presence of CFO. Section III treats the derivations of the SNR estimators for the data-aided scenario in the presence of a Rayleigh fading channel. Section IV considers the estimators for non-data-aided case and in Section V, we will discuss the simulation results for various estimators and overall estimator performance in terms of mean-squared error and the CRB. The correspondence then concludes in Section VI.

II. System Model

Consider a Rayleigh fading communication system employing binary FSK modulation, where a block of data with k symbols undergoes symbol-rate fading. The received signal observed at the receiver end is given as

$$r(t) = \sqrt{E_s}\alpha(t)\exp\left(j2\pi(f_c + f_m + \Delta f)t + \theta\right) + n(t), \quad 0 \le t \le T, \quad m \in \{1,2\} \tag{1}$$

where E_s is the signal power, T is the symbol time, f_c is the carrier frequency, and f_m is the BFSK frequency corresponding to the message signal. The shift in the carrier frequency at the receiver is denoted as Δf and θ is the unknown carrier phase. Without the loss of generality we will set $\theta = 0$, since we are dealing with the noncoherent receiver. The noise at the receiver is $n(t)$, which is AWGN and $\alpha(t)$ is the Rayleigh fading envelope. Thus, the integrator output, matched to the transmitted signal S_m is given as

$$v_m = \int_0^T r(t)\sqrt{E_s}\exp\left(-j2\pi(f_c + f_m)t\right)dt \tag{2}$$

where we get the signal part, after simplifying the above equation, as

$$v_{ms} = P\alpha\left[\frac{1 - \exp(-j2\pi\Delta fT)}{j2\pi(m-1) + j2\pi\Delta fT}\right], \quad m \in \{1,2\} \tag{3}$$

where $P = \frac{E_s T}{2}$. For the sake of simplicity, we assume that the average symbol energy is unity, i.e., $P = 1$, and thus the signal output after the

Manuscript received October 26, 2010; revised January 25, 2011; accepted March 14, 2011. Date of publication March 22, 2011; date of current version June 15, 2011. The associate editor coordinating the review of this manuscript and approving it for publication was Dr. Mathini Sellathurai. The authors gratefully acknowledge support for this research from the National Science Foundation under Grant CNS-0721296.

The authors are with the School of Electrical and Computer Engineering, Georgia Institute of Technology, Atlanta, GA, 30332 USA (e-mail: alihassan@gatech.edu; mai@ece.gatech.edu).

Color versions of one or more of the figures in this correspondence are available online at http://ieeexplore.ieee.org.

Digital Object Identifier 10.1109/TSP.2011.2131137

square law detector for the BFSK receiver having a frequency carrier shift of Δf is given as

$$x_{m,i} = \left| \alpha_i \left[\frac{1 - \exp(-j2\pi\rho)}{j2\pi(m-1) + j2\pi\rho} \right] + n_{m,i} \right|^2, \quad m \in \{1, 2\} \quad (4)$$

where $\rho = \Delta f T$ is the normalized frequency error, $|.|$ is the magnitude operator, and the CFO factors in both branches are given as

$$A_m = \left| \frac{1 - \exp(-j2\pi\rho)}{j2\pi(m-1) + j2\pi\rho} \right|^2, \quad m \in \{1, 2\}. \quad (5)$$

The received symbols from 2 branches are denoted by $x_{m,i}$, where the first index m denotes the branch index and the second index i is the time index such that $i = \{1, 2, \ldots, k\}$; k being the packet length. The channel gains, α_i, and the noise elements, n_i, are zero mean complex Gaussian random variables with variance of $\frac{S}{2}$ and $\frac{N}{2}$ per real dimension, respectively. We can express $\mathbf{x}_i = [x_{1,i}\ x_{2,i}]^T$ to be the received signal vector at time i. Since we assumed that the average symbol energy is unity, the expected energy of the ith received symbol is given as S. Thus, the signal-to-noise ratio is given by $\gamma = \frac{S}{N}$. Our interest is to find the estimate of the average SNR using the observed data, after the square law detector but it can be seen that the factor A_m in (5) will reduce the signal power if $\rho \neq 0$. Thus, in this correspondence, we will try to estimate the CFO, ρ, and treat it as a nuisance parameter which is essential to estimate the actual parameter of interest namely, the signal to noise ratio. Throughout the correspondence, we assume perfect timing recovery at the receiver.

III. Data Aided Estimation

In this section, we derive the SNR estimator for the BFSK receiver in the presence of CFO, while having full knowledge of the transmitted data. Therefore, without the loss of generality, we assume that all the transmitted symbols are identical, and correspond to frequency f_1. We drop the time index i for the ease of notation and use the received data in one symbol period, because the received symbols are independent at each time slot. From (4), it can be seen that the signal power is reduced by the CFO factor, A_1, in the upper branch (x_1) and there is also a signal spill which introduces some part of signal power in the lower branch, given by A_2, where these factors are given as $A_1 = \frac{\sin^2(\pi\rho)}{(\pi\rho)^2}$ and $A_2 = \frac{\sin^2(\pi\rho)}{(\pi(1+\rho))^2}$. Because of the signal leakage in both of the branches, the two branches no longer remain orthogonal and hence there exists a correlation between the outputs x_1 and x_2, given by the cross-correlation coefficient as

$$\xi = \frac{2A_1A_2S^2 + SN(A_1 + A2) + N^2}{(A_1S + N)(A_2S + N)} - 1. \quad (6)$$

From (4), as α and n are zero-mean complex Gaussian, therefore, the probability density function (PDF) of both the branches become exponential after passing through the envelope detector. As shown in [7], the best performance of SNR estimator, in terms of CRB, can be obtained if the likelihood function for the received data is maximized after the envelope detector, i.e., the best estimator is obtained if the input data to the SNR estimator is the vector $\mathbf{x}$. However, there exists a correlation between the elements of $\mathbf{x}$, because of which the joint PDF of the received signal vector is given by Downton's bivariate exponential distribution [12], containing a modified Bessel function. The presence of modified Bessel function makes the problem at hand very tedious to solve analytically. However, a reasonable solution can be obtained if the input data to the estimator is the difference between x_1 and x_2, which is also available in the BFSK receiver. Thus, we use the Laplace distribution [13], which is obtained by taking the difference of two exponential random variables as $y = x_1 - x_2$. In order to further simplify the PDF expression, we define the following: $\mu = A_1 + A_2$, $\nu = A_1 - A_2$, and $\phi = \sqrt{4N^2 + 4\mu SN + \nu^2 S^2}$. Thus, the PDF of y is given as

$$p_y(y) = \frac{2}{4\sigma_1^2\sigma_2^2(1-\xi)\eta} \exp\left(-\frac{\alpha y}{4}\right), \quad y \geq 0 \quad (7)$$

where $2\sigma_m^2 = A_m S + N, m \in \{1, 2\}, \eta = \frac{2\phi}{N^2 + \mu SN}$, and $\alpha = \frac{8}{\nu S + \phi}$. It can be seen from (7), that a closed-form solution will be prohibitive if we try to maximize the log-likelihood function of (7) with respect to three parameters namely S, N, and ρ. Specifically the CFO parameter is very difficult to solve analytically through this optimization problem. A solution can be obtained if we somehow know the CFO factor, ρ. In the following subsection, we estimate ρ using the moments based method, which turns out to be a very accurate estimate, especially at high SNR. Then we will show how the estimate of CFO can help in estimating the SNR using the conventional ML method.

A. Method of Moments Approach

In the method of moments (MM) approach, we use the first order self and cross statistics of the received data to estimate the CFO, which will subsequently be used in the estimation of SNR. In this case, the first order statistics obtained from both the branches are as follows:

$$\mathbb{E}\{x_m\} = A_m S + N, \quad m \in \{1, 2\} \quad (8)$$

and the first cross-moment is given as

$$\mathbb{E}\{x_1 x_2\} = 2A_1A_2S^2 + SN(A_1 + A_2) + N^2. \quad (9)$$

In practice, we replace the ensemble averages in previous equations with those of time averages, i.e., $\mathbb{E}\{x\} \approx \frac{1}{k}\sum_{i=1}^{k} x_i$. Hence, we denote the time averages as $\mathbb{E}\{x_1\} := X$, $\mathbb{E}\{x_2\} := Y$, and $\mathbb{E}\{x_1 x_2\} := Z$. We also let $\hat{A}_1 = A_1 S$ and $\hat{A}_2 = A_2 S$, then (8) and (9) can be solved simultaneously to get the estimate of the noise power, N, as

$$\hat{N} = \frac{1}{2}\left(X + Y - \sqrt{(X^2 - 6XY + Y^2 + 4Z)}\right), \quad (10)$$

and the estimates of $\hat{A}_1$ and $\hat{A}_2$ are given as $\hat{\hat{A}}_1 = X - \hat{N}$ and $\hat{\hat{A}}_2 = Y - \hat{N}$. Finally, we get the estimates of ρ and then the signal power, as given by following equations:

$$\hat{\rho} = \frac{\hat{\hat{A}}_2 + \sqrt{\hat{\hat{A}}_1 \hat{\hat{A}}_2}}{\hat{\hat{A}}_1 - \hat{\hat{A}}_2} \quad (11)$$

$$\hat{S} = \frac{\hat{\hat{A}}_1}{\hat{A}_1} = \hat{\hat{A}}_1 \left(\frac{\pi\hat{\rho}}{\sin(\pi\hat{\rho})}\right)^2. \quad (12)$$

It will be shown in the results section that the SNR estimate resulting from (12) and (10) shows a high mean squared error in the high SNR region. However, the estimate of ρ is accurate to a high precision for SNR $\geq$ 7 dB.

B. Maximum-Likelihood Approach

In the ML approach, we assume the knowledge of CFO, which we get from the MM estimator in the previous subsection. Based upon the known value of ρ, we can treat μ and ν in (7) as constant parameters. Thus, the log-likelihood of the k symbols, y_i, $i = \{1, 2, \ldots, k\}$, is given as

$$\Lambda(\mathbf{y}; S, N|\rho) = -\frac{k}{2}\log\phi^2 - \frac{2}{(\nu S + \phi)}\sum_{i=1}^{k} y_i. \quad (13)$$

Maximizing the above likelihood with respect to S and N again prohibits a closed-form expression for the estimates of signal power and noise power. However, it will be shown in the results section that the estimate of the CFO and hence the noise power from the MM estimator is fairly accurate. Therefore, we can use the estimate of the noise power from the MM estimator to derive the ML estimator.

Based on the above discussions, the log-likelihood function can be further simplified by using SNR γ, i.e., $\frac{S}{N}$, and the noise, N, as the parameters of interest. Thus, we get

$$\Lambda(\mathbf{y};\gamma|N) = -k\log N - k\log\tilde{\phi} - \frac{2}{N(\nu\gamma+\tilde{\phi})}\sum_{i=1}^{k} y_i, \quad (14)$$

where $\tilde{\phi} = \sqrt{4+4\mu\gamma+\nu^2\gamma^2}$. Finding the maxima of the log-likelihood with respect to γ gives the following estimate of SNR:

$$\hat{\gamma} = \frac{\left(\sum_{i=1}^{k} y_i\right)^2/(k\hat{N}) - k\hat{N}}{\nu\sum_{i=1}^{k} y_i + \mu k\hat{N}}. \quad (15)$$

C. Cramér–Rao Lower Bound

The CRB, which is the benchmark on the variance of an estimator, is a function of the Fisher information, $F(\gamma)$, [14], and is given as $\text{CRB} = \frac{1}{F(\gamma)}$, where $F(\gamma)$ is given as

$$F(\gamma) = -\mathbb{E}\left\{\frac{\partial^2\Lambda}{\partial\gamma^2}\right\}. \quad (16)$$

Thus twice differentiating (14) with respect to γ and taking the expectation gives the following Fisher information:

$$F(\gamma) = \frac{1}{\tilde{\phi}^4}\left[k\left\{-\mu^2\tilde{\phi}^2 + 2(2\nu+\mu^2\gamma)^2 - \frac{\psi}{(\phi+\mu\gamma)^3}\right\}\right] \quad (17)$$

where $\psi = 2\mu\tilde{\phi}\gamma(\tilde{\phi}(\mu\tilde{\phi}+6\nu)+2\mu\gamma(\mu\tilde{\phi}+\nu)+\mu^3\gamma^2)(2\nu+\mu(\tilde{\phi}+\mu\gamma))$.

IV. Non-Data-Aided Estimation

In this section, we derive the MM and ML estimators for the non-data-aided scenario where we assume the equally likely probability of the transmission of the data symbols. We follow the same approach of finding $\hat{\rho}$ and $\hat{N}$ from the MM estimator and then use these estimates to find the ML SNR estimator.

A. Method of Moment Estimator

For the NDA case, we assume that $\mathbb{P}\{\text{signal} \in x_1\} = \mathbb{P}\{\text{signal} \in x_2\} = \frac{1}{2}$. Hence, the average value of both branches remains the same. Thus, we use the following statistics of the data in order to estimate the CFO:

$$\mathbb{E}\{x_m\} = \frac{1}{2}[\tilde{A}_1 + \tilde{A}_2 + 2N], \quad m \in \{1,2\} \quad (18)$$

$$\mathbb{E}\{x_1x_2\} = 2\tilde{A}_1\tilde{A}_2 + N(\tilde{A}_1+\tilde{A}_2) + N^2. \quad (19)$$

Since we need three linearly independent equations in order to get the estimates of three parameters, we use the following vector formulation of the received data:

$$\mathbf{Z} = (\mathbb{E}\{\mathbf{x}\})(\mathbb{E}\{\mathbf{x}\})^T\left(\mathbb{E}\{\mathbf{x}\mathbf{x}^T\}\right)^{-1} \quad (20)$$

where $\mathbb{E}\{\mathbf{x}\} = [\mathbb{E}\{x_1\}\,\mathbb{E}\{x_2\}]^T$. Thus, $\mathbb{E}\{\mathbf{x}\}\mathbb{E}\{\mathbf{x}\}^T$ is given as

$$\mathbb{E}\{\mathbf{x}\}\mathbb{E}\{\mathbf{x}\}^T = \frac{1}{4}[\tilde{A}_1 + \tilde{A}_2 + 2N]^2\mathbf{1}_2 \quad (21)$$

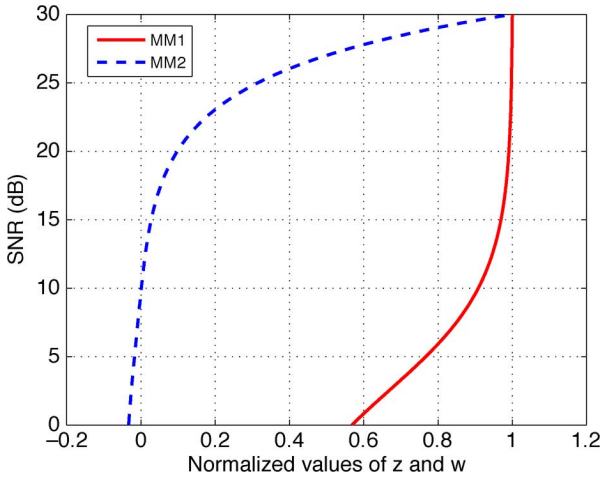

Fig. 1. Behavior of MM1 and MM2 estimators for non-data-aided case.

where $\mathbf{1}_2$ is a 2×2 matrix of all ones. The autocorrelation matrix of the received data, given by $E\{\mathbf{x}_m\mathbf{x}_m^T\}$, contains $E\{x_m^2\}$ on the main diagonal given as

$$\mathbb{E}\{x_m^2\} = \left(\tilde{A}_1^2 + \tilde{A}_2^2\right) + 2N(\tilde{A}_1+\tilde{A}_2) + 2N^2, \quad m \in \{1,2\} \quad (22)$$

while the off-diagonal elements are given as $\mathbb{E}\{x_1x_2\}$, which are given by (19). Thus, taking the inverse of this matrix and multiplying it with (21) gives us the following $\mathbf{Z}$:

$$\mathbf{Z} = \frac{(\tilde{A}_1+\tilde{A}_2+2N)^2}{4\left[(\tilde{A}_1+\tilde{A}_2)^2 + 3N(\tilde{A}_1+\tilde{A}_2) + 3N^2\right]}\mathbf{1}_2. \quad (23)$$

Since the resulting $\mathbf{Z}$ from the above equation contains identical elements at each location of 2×2 matrix, therefore, we can select only one of the elements from $\mathbf{Z}$. As in the previous case, we let $\mathbb{E}\{x_m\} := X$, then any $z \in Z$ can be written as

$$z = \frac{X^2}{(2X-2N)^2 + 3N(2X-2N) + 3N^2} \quad (24)$$

which gives the estimate of the noise power N as

$$\hat{N} = X[1 - \sqrt{1/z - 3}]. \quad (25)$$

Let us denote this estimator (resulting from the statistic z) as MM1. We have plotted the results from (24) for the computed statistic, z, against the SNR, γ, in Fig. 1 for a CFO factor $\rho = 0.1$. The curve in the figure exhibits smooth monotone behavior for low values of SNR, i.e., when SNR $\in [0, 10]$. Thus, the estimator performance is anticipated to be good in this SNR region. However, as the SNR increases, the curve appears to approach a vertical asymptote. This implies that a very small change in the computed statistics of data would cause a huge variation in the estimated value of SNR. Hence, this approach will suffer in the estimation of high SNR values. Therefore, this approach of MM1 can be used as an NDA approach for SNR estimation for low SNR values.

In order to design an estimator which performs better at high SNR values, we consider another statistic of the received data

$$\mathbb{E}\left\{x_1x_2^2\right\} = N(3NX - 2X^2) - Y(2N - 3X) \quad (26)$$

where, as before, $Y := \mathbb{E}\{x_1 x_2\}$. Let $W := \frac{\mathbb{E}\{x_1 x_2^2\}}{\mathbb{E}\{x_1^2\}}$, then an estimate of the noise power in terms of statistic W is given as

$$\hat{N} = \frac{1}{W - 3X}\left[WX - X^2 - Y + \sqrt{f(W,X,Y)}\right] \tag{27}$$

where $f = X^4 - 7X^2Y + Y^2 + W^2(Y - 3X^2) + 2W(5X^3 - XY)$. We denote this estimator as MM2. The estimator characteristics are also plotted in Fig. 1. It can be seen that this estimator would not estimate accurately in the low SNR regime because of the vertical asymptote. However, the estimator performance is likely to be good in the high SNR region since the estimator characteristic exhibits almost linear behavior. Hence, we can use MM2 for the NDA estimation of SNR in the high SNR region.

For the estimate of the CFO, we notice from the definitions of A_1 and A_2 that, $\frac{A_1 A_2}{(A_1+A_2)^2} = \left(\frac{\rho(1+\rho)}{\rho^2+(1+\rho)^2}\right)^2$. If we denote this ratio of CFO factors as β, then ρ can be given as a function of β as follows:

$$\rho = \frac{1 - 2\sqrt{\beta} - \sqrt{1 - 4\beta}}{2(2\sqrt{\beta} - 1)}. \tag{28}$$

We can calculate β from (18) and (19), which gives $\beta = \frac{Y - \hat{N}(2X - 2\hat{N}) - \hat{N}^2}{2(2X - 2\hat{N})^2}$, where $\hat{N}$ can be found by either using MM1 or MM2. Finally the signal power is given as

$$\hat{S} = \frac{2X - 2\hat{N}}{\hat{A}_1 + \hat{A}_2} \tag{29}$$

where $\hat{A}_1$ and $\hat{A}_2$ can be computed using the estimate of ρ from (28).

B. Maximum-Likelihood Approach

Using the difference of random variables, $y = x_1 - x_2$, as done in the previous section and assuming equally likely probability of transmitted symbols, the PDF of the received symbols is given as

$$p_y(y) = \frac{1}{4}\left[\frac{1}{\sqrt{(\hat{\sigma}_2^2 - \hat{\sigma}_1^2)^2 + 4\hat{\sigma}_1^2\hat{\sigma}_2^2(1-\xi)}} \exp\left(-\frac{1}{4}\alpha^+|y|\right) + \frac{1}{\sqrt{(\tilde{\sigma}_2^2 - \tilde{\sigma}_1^2)^2 + 4\tilde{\sigma}_1^2\tilde{\sigma}_2^2(1-\xi)}} \exp\left(-\frac{1}{4}\alpha^-|y|\right)\right] \tag{30}$$

where $2\hat{\sigma}_1^2 = 2\tilde{\sigma}_2^2 = A_1 S + N$, $2\hat{\sigma}_2^2 = 2\tilde{\sigma}_1^2 = A_2 S + N$,

$$\alpha^+ = \frac{\sqrt{(\hat{\sigma}_2^2 - \hat{\sigma}_1^2)^2 + 4\hat{\sigma}_1^2\hat{\sigma}_2^2(1-\xi)} + \hat{\sigma}_2^2 - \hat{\sigma}_1^2}{\hat{\sigma}_1^2\hat{\sigma}_2^2(1-\xi)}, \tag{31}$$

and

$$\alpha^- = \frac{\sqrt{(\tilde{\sigma}_2^2 - \tilde{\sigma}_1^2)^2 + 4\tilde{\sigma}_1^2\tilde{\sigma}_2^2(1-\xi)} + \tilde{\sigma}_2^2 - \tilde{\sigma}_1^2}{\tilde{\sigma}_1^2\tilde{\sigma}_2^2(1-\xi)}. \tag{32}$$

However, $\alpha^+ = \alpha^-$ and thus both terms are simply added up to give the PDF of the received symbols as

$$p_y(y) = \frac{1}{2\hat{\sigma}_1^2\hat{\sigma}_2^2(1-\xi)\eta} \exp\left(-\frac{\alpha|y|}{4}\right) \tag{33}$$

which is the same PDF as for the data-aided case in (7), with the only difference that the absolute of the data will be used now. Hence, we use the same approach as in the Section III-B. The likelihood and hence the resulting estimates of the SNR follow from (14) and (15), respectively. Even there is no change in the CRB, because the likelihood of both the schemes is the same and also $\mathbb{E}\{y\}, y \geq 0$ for the DA case is the same as $\mathbb{E}|y|$ for the NDA case. The Fisher Information and hence the CRB also remains equal.

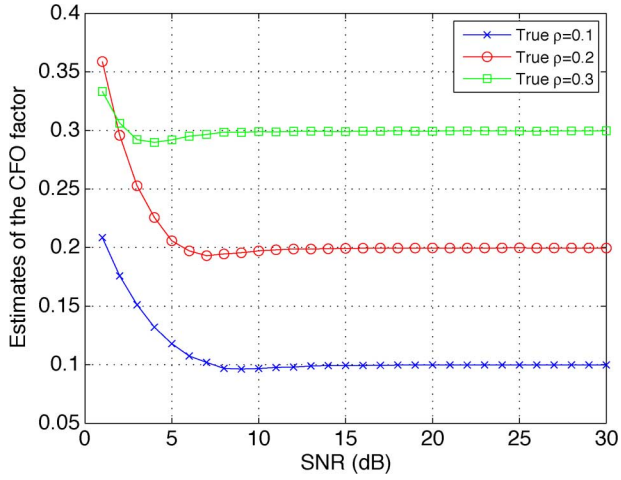

Fig. 2. Estimation of ρ by MM estimator for $k = 1000$ in the data-aided scenario.

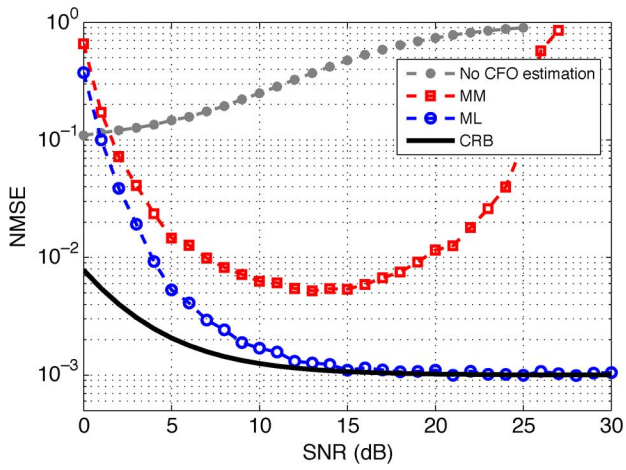

Fig. 3. NMSE plot for SNR estimation for the data-aided scenario for $k = 1000$.

V. Simulation Results

In this section, we compare the normalized mean-square error (NMSE) (normalized with respect to the square of the true value of the SNR) of the estimators using simulations for both the data-aided and non-data-aided scenarios for a packet length, $k = 1000$, averaged over 20 000 trials. For the data-aided scenario, Fig. 2 shows the estimates the CFO factor, ρ, using the MM approach for the DA case. It can be seen that the estimate of CFO is highly accurate for SNR $\geq$ 7 dB. Fig. 3 shows the NMSE for the SNR estimation resulting from both the MM and the ML estimator. In the "No CFO estimation" case, the SNR is estimated without estimating the CFO from the algorithm derived in [8]. We observe that as the SNR increases, the leakage in the lower branch increases and consequently the error in the estimation increases. It can also be noticed that the MM estimator works well for the SNR estimation at low values of SNR. However, it suffers in the high SNR region due to a higher bias for high values of signal power in this range. The same cup shaped curve of MM estimator can also be seen in [15]. From the MM estimator, we know that the estimate of ρ is quite accurate and this estimate also depends on the noise estimate from (10), (11), hence we can use these estimates to derive the ML algorithm and the resulting curve in Fig. 3 shows that the NMSE is quite small if we use the estimates from the MM estimator. The CRB is also plotted

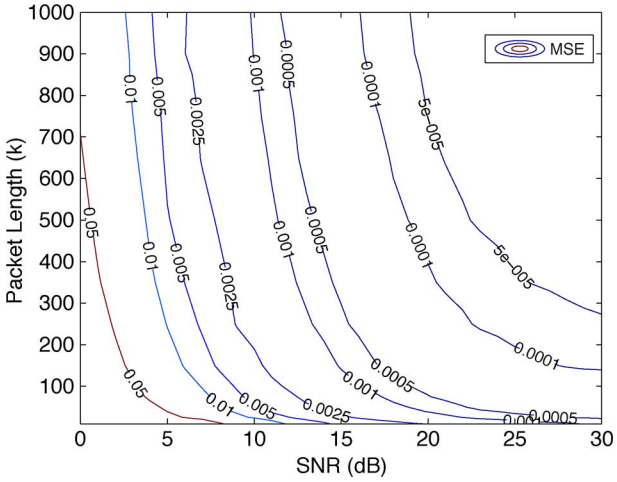

Fig. 4. MSE contour plot for different packet lengths in the MM estimation of CFO for the data-aided case.

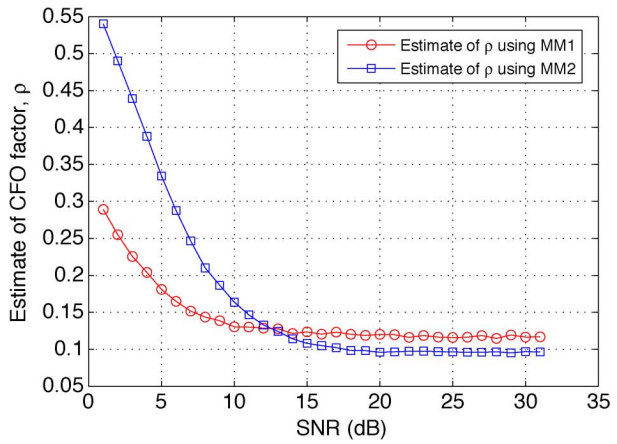

Fig. 5. Estimation of ρ by NDA MM estimators; true value of $\rho = 0.1$.

to compare the results. The high error in the low SNR region of ML estimator is due to two facts: 1) bad estimates of ρ in MM, 2) at low SNR, the condition of $y \geq 0$ is not always satisfied in the PDF from (7). However, the ML estimator shows good results at high SNR.

The above simulation results were for a packet length of $k = 1000$. However, it is interesting to note the performance of the estimate of ρ even at small packet lengths. The contour plot in Fig. 4 shows the MSE of the estimation of CFO factor for various values of packet lengths. It can be seen that even if the packet length is small, we can get good estimates of ρ, which can be used in the ML estimator to accurately estimate the SNR.

Fig. 5 shows the estimation of the CFO factor for the non-data-aided case using both the MM1 and MM2 estimator for a packet length of 1000. It be seen that the MM1 estimator performs better at low SNR as compared to the MM2 estimator. However, in the high SNR region, the MM2 estimator gives a very accurate estimate of ρ, which is evident from the discussions in Section IV-A and Fig. 1. However, the NMSE at high SNR for both the estimators is very large (and is not plotted in Fig. 6), hence both of them cannot be used for SNR estimation at high values of SNR. At low SNR, the MM1 estimator gives a fairly better performance as can be seen from Fig. 6. We have plotted the NMSE for the NDA ML estimator using both the estimates from MM1 and MM2. It can be seen that using the estimates from MM1 results in a better performance in low SNR region as expected, while the NMSE is higher for the

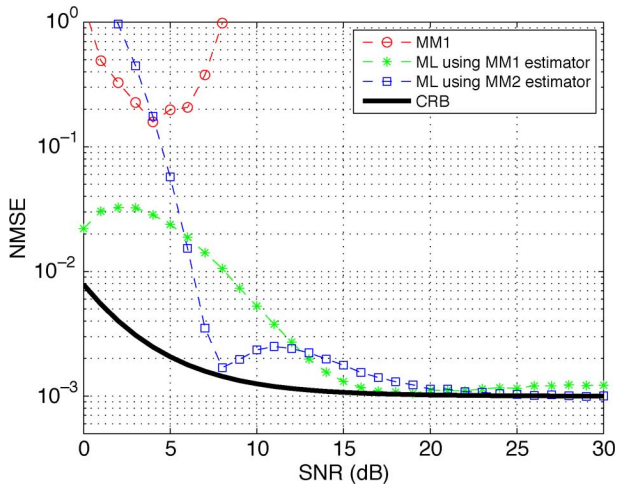

Fig. 6. NMSE for SNR estimators for non-data-aided case; $k = 1000$.

MM2 estimator in the same SNR range. However, an interesting result arises in the high SNR regime. We observe that the NMSE performance is little better for MM2-ML estimator, however the performance is almost the same for both the NDA-MM1 and NDA-MM2 estimators, and the performance reaches to that of the CRB at very high values of SNR.

VI. Conclusion

In this correspondence, we have studied the problem of estimating the SNR in the presence of a CFO. We have derived both the data aided and non-data-aided estimators for the Rayleigh fading channel and have derived method of moments estimator and the maximum likelihood estimator for each case. Concerning the difficulty of the CFO estimation problem (in terms of its nonlinearity), we have shown that the estimates of CFO can be found using the MM estimators, which can then be used to derive the ML estimators, which give accurate estimates of the SNR at various high and low SNR scenarios.

References

[1] S. A. Hassan, Y. G. Li, P. S. S. Wang, and M. W. Green, "A full rate dual relay cooperative approach for wireless systems," *J. Commun. Netw. (JCN)*, vol. 12, no. 5, pp. 442–448, Oct. 2010.

[2] D. R. Pauluzzi and N. C. Beaulieu, "A comparison of SNR estimation techniques for the AWGN channel," *IEEE Trans. Commun.*, vol. 48, no. 10, pp. 1681–1691, Oct. 2000.

[3] Y. Chen and N. C. Beaulieu, "An approximate maximum likelihood estimator for SNR jointly using pilot and data symbols," *IEEE Lett. Commun.*, vol. 9, no. 6, pp. 517–519, Jun. 2005.

[4] A. Ramesh, A. Chockalingam, and L. B. Milstein, "SNR estimation in generalized fading channels and its applications to turbo decoding," in *Proc. IEEE ICC*, Helsinki, Finland, Jun. 2001, pp. 1094–1098.

[5] A. Ramesh, A. Chockalingam, and L. B. Milstein, "SNR estimation in Nakagami-m fading with diversity combining and its applications to turbo decoding," *IEEE Trans. Commun.*, vol. 50, no. 11, pp. 1719–1724, Nov. 2002.

[6] T. Ertas and E. Dilaveroglu, "Low SNR asymptote of CRB on SNR estimates for BPSK in Nakagami-m fading channels with diversity combining," *IEEE Electron. Lett.*, vol. 39, no. 23, pp. 1680–1682, Nov. 2003, DOI: 10.1049/el:20031057 .

[7] E. Dilaveroglu and T. Ertas, "CRBs and MLEs for SNR estimation on non coherent BFSK signals in Rayleigh fading," *IEEE Electron. Lett.*, vol. 41, no. 2, pp. 79–80, Jan. 2005.

[8] S. A. Hassan and M. A. Ingram, "SNR estimation for a non-coherent M-FSK receiver in Rayleigh fading environment," presented at the IEEE Int. Conf. Communications (ICC), Cape Town, South Africa, May 23–27, 2010.

[9] S. A. Hassan and M. A. Ingram, "SNR estimation for a non-coherent M-FSK receiver in a slow flat fading environment," presented at the IEEE Int. Conf. Communications (ICC), Cape Town, South Africa, May 23–27, 2010.

[10] S. Hinedi, M. K. Simon, and D. Raphaeli, "The performance of non-coherent orthogonal M-FSK in the presence of timing and frequency errors," *IEEE Trans. Commun.*, vol. 43, pp. 922–933, Feb. 1995.
[11] M. Ju and I. M. Kim, "Error probabilities of non-coherent and coherent FSK in the in the presence of frequency and phase offsets for two-hop relay networks," *IEEE Trans. Commun.*, vol. 57, no. 8, pp. 2244–2250, Aug. 2009.
[12] F. Downton, "Bivariate exponential distributions in reliability theory," *J. Royal Statistical Soc., B*, vol. 32, pp. 408–417, 1970.
[13] M. K. Simon, *Probability Distributions Involving Gaussian Random Variables: A Handbook for Engineers and Scientists*. New York: Springer, 2002.
[14] S. M. Kay, *Fundamentals of Statistical Signal Processing: Estimation Theory*. Englewood Cliffs, NJ: Prentice-Hall, 1993.
[15] S. A. Hassan and M. A. Ingram, "SNR estimation for a non-coherent binary frequency shift keying receiver," presented at the IEEE Global Commum. Conf. (GLOBECOM), Honolulu, HI, Nov. 30–Dec. 4, 2009.

Stochastic Multiple Stream Decoding of Cortex Codes

Matthieu Arzel, Cyril Lahuec, Christophe Jego, Warren J. Gross, and Yvain Bruned

***Abstract*—Being one of the most efficient solutions to implement forward error correction (FEC) decoders based on belief propagation, stochastic processing is thus a method worthy of consideration when addressing the decoding of emerging codes such as Cortex codes. This code family offers short block codes with large Hamming distances. Unfortunately, their construction introduces many hidden variables making them difficult to be efficiently decoded with digital circuits implementing the Sum-Product algorithm. With the introduction of multiple stochastic streams, the proposed solution alleviates the hidden variables problem thus yielding decoding performances close to optimal. Morevover, this new stochastic architecture is more efficient in terms of complexity-throughput ratio compared to recently published stochastic decoders using either edge or tracking forecast memories.**

***Index Terms*—Cortex codes, stochastic decoding, sum-product algorithm.**

I. Introduction

Turbo [1] and LDPC [2], [3] codes allow near optimal decoding performance for codes of block lengths larger than a few hundreds of bits. However, these code families are not adapted to smaller blocks. Also based on iterative encoding and interleaving stages, Cortex codes [4], [5] were invented for this purpose. They are asymptotically good [6] and possess interesting properties such as a systematic construction of self-dual codes [4] and the possibility to associate every type-II self dual code with a Cortex code [7]. Although the Cortex construction offers short codes with large Hamming distances, they are generally difficult to decode with usual digital implementation techniques [7], [8] due to the complexity of the decoding graphs and the large number of hidden variables. The first efficient Cortex decoder was implemented for codes based on the (4,2,2) Hadamard code with analog circuits [9] applying the Sum-Product Algorithm (SPA). But is it possible to achieve such results with digital circuits? The state-of-the-art digital implementations of the original SPA for LDPC codes consist of different optimized versions of the Min-Sum solution provided in [10], with the exception of stochastic circuits originally proposed in [11]. Stochastic decoders have been so optimized that they provide some of the most efficient implementations of LDPC decoders [12].

Principles of stochastic computation were elaborated in the 1960s [13], [14] as a method to carry out complex operations with a low hardware complexity. The probabilities are converted into streams of stochastic bits using Bernoulli sequences in which the information is given by the statistics of the bit streams. Complex arithmetic operations on probabilities such as multiplication and division are transformed into operations on bits using elementary logic gates. Stochastic decoder architectures are designed with low computational complexity and a high level of parallelism [15], [16] achieving high throughputs [12], [17], [18]. Moreover, stochastic decoding is of high interest for low-power decoders [19] and fault-tolerant nanoscale circuits [20].

The main goal of this paper is to show that Cortex codes can be efficiently decoded, despite the complexity of their decoding graphs, by state-of-the-art techniques, i.e., stochastic processing. An original idea is also introduced to reduce the number of clock cycles required to decode one codeword and to replace the edge memories (EMs) [17] by simple deterministic shufflers. The paper is organized as follows. Section II summarizes the principles of Cortex codes. A stochastic decoder architecture is presented to deal with them in Section III. This architecture is then compared with analog SPA and digital Min-Sum counterparts in terms of decoding performance in Section IV. Section V concludes the paper.

II. Cortex Codes

A. Design Principles

Cortex codes were originally designed as systematic codes of rate one half [4]. As shown in Fig. 1, the systematic symbols are grouped in frames of k symbols denoted by x_i. Any frame $\mathbf{x}$ is sliced into p parts of same length m. Each sub-frame, or slice, is independently encoded using a component encoder C_j^0 of rate one half. The resulting redundant symbols are grouped into a frame of length k denoted by $\mathbf{v^0}$. Then, this frame is interleaved over its full-length k. This slicing-encoding-grouping-interleaving scheme is iterated s times. Finally, the resulting frame $\mathbf{v^s}$ is again sliced and encoded to yield the redundant frame $\mathbf{r}$ of length k. If the same self-dual code is used for any component code, then, depending on constraints on the interleavers [21], the resulting Cortex code is also self-dual. Thus, codes with Hamming distances multiple of two or four are built. Using this Cortex construction, many known and new extremal short codes can be built, as shown in [7].

B. C4 Codes

Whereas the Cortex codes generally used the extended (8,4,4) Hamming code as component code, other codes can be used. For instance, in [9] the basic (4,2,2) Hadamard code, the smallest self-dual code, was

Manuscript received October 13, 2010; revised February 02, 2011; accepted March 15, 2011. Date of publication April 07, 2011; date of current version June 15, 2011. The associate editor coordinating the review of this manuscript and approving it for publication was Prof. Jarmo Takala.

M. Arzel and C. Lahuec are with the Institut Telecom/Telecom Bretagne, CNRS Lab-STICC UMR 3192, Technopole Brest-Iroise F-29238 BREST Cedex 3, France (e-mail: qt.dong@telecom-bretagne.eu; matthieu.arzel@telecom-bretagne.eu).

C. Jego is with the CNRS IMS, UMR 5218, F-33405 Talence Cedex (e-mail: christophe.jego@ims-bordeaux.fr).

W. J. Gross is with the Department of Electrical and Computer Engineering, McGill University, Montreal, QC H3A 2A7, Canada (e-mail: wjgross@ece.mcgill.ca).

Y. Bruned is with the ENS Cachan/Bretagne, F-35170 Bruz, France (e-mail: Yvain.Bruned@eleves.bretagne.ens-cachan.fr).

Color versions of one or more of the figures in this paper are available online at http://ieeexplore.ieee.org.

Digital Object Identifier 10.1109/TSP.2011.2138699